Molecular Therapy
Methods & Clinical Development
Original Article

Reduced rAAV interference enhances rcAAV detection sensitivity

Ming Yang,[1,2,9] Sana Shaheen,[1,9] Keying Yang,[1] Xuxia Gao,[1] Kaiwen Wu,[3] Xiangying Zhu,[4] Qian Kang,[5] Lu Wang,[5] Farhid Hemmatzadeh,[6] Qingyun Zheng,[1,7] Chen Ling,[1,8] Liqing Zhu,[3,5] and Bicui Zhan[2]

[1]State Key Laboratory of Genetics and Development of Complex Phenotypes and Engineering Research Center of Gene Technology (Ministry of Education), School of Life Sciences, Zhongshan Hospital, Fudan University, Shanghai 200438, China; [2]Department of Clinical Laboratory, Hangzhou TCM Hospital Affiliated to Zhejiang Chinese Medical University, Hangzhou, Zhejiang 310007, China; [3]Department of Clinical Laboratory, the First Affiliated Hospital of Wenzhou Medical University, Wenzhou, Zhejiang 325000, China; [4]Zhejiang Hengyu Biological Technology Co., Ltd., Jiaxing, Zhejiang Province 314113, China; [5]Department of Clinical Laboratory, Peking University Cancer Hospital & Institute, Beijing 100142, China; [6]School of Animal and Veterinary Sciences, The University of Adelaide, Adelaide, SA 5371, Australia; [7]Nuffield Laboratory of Ophthalmology, Department of Clinical Neurosciences, University of Oxford, OX3 9DU Oxford, UK; [8]Shanghai Key Laboratory of Gene Editing and Cell Therapy for Rare Diseases, Fudan University, Shanghai 200031, China

Replication-competent adeno-associated virus (rcAAV) content is a crucial contaminant in the process of recombinant adeno-associated virus (rAAV) production in gene therapy products, from preclinical to clinical stages. The gold standard for qPCR-based quantification of rcAAV involves co-infecting HEK293 cells with recombinant adenovirus (rAd) and rAAV samples, followed by amplification and qPCR analysis of both the rcAAV and rAAV genomes. Here, we reported that the presence of large quantity of rAAV interferes with accurate rcAAV detection, leading to false-negative results. In addition, we present a CRISPR-based approach to improve rcAAV detection, where SpCas9 was overexpressed in HEK293 cells and single-guide RNA (sgRNA) was delivered via rAd5 to cleave the rAAV genome. The assay detected as few as 3E2 vector genomes (vg) of rcAAV, whereas the traditional method using the same sample batch failed to detect such low levels. This study not only expands our knowledge of adeno-associated virus (AAV) biology but also highlights a CRISPR-based assay that improves the sensitivity of rcAAV detection.

INTRODUCTION

Recombinant adeno-associated virus (rAAV) is a highly effective gene delivery vector with low immunogenicity and sustained transduction and has been the basis for eight Food and Drug Administration (FDA) and European Medicines Agency (EMA)-approved therapeutics.[1] It is not only a powerful gene editing tool in laboratory research[2] but also involved in 214 ongoing clinical trials worldwide. While rAAV-based therapies have shown great promise, severe adverse reactions have been reported in some patients during clinical trials. The potential immunotoxicity caused by replication-competent adeno-associated virus (rcAAV) has been a significant concern.[3,4] Studies have shown that rcAAV activates specific $CD8^+$ T cells in patients, potentially contributing to immunotoxicity in transduced tissues, leading to the degradation of adeno-associated virus (AAV) gene therapy vectors and impairing the long-term expression of transgenes. Furthermore, because many individuals have prior exposure to wild-type AAV and/or adenoviruses, subsequent infection with rcAAV could trigger a heightened immune response and promote the replication of wild-type AAV.[5,6] For these reasons, regulatory agencies mandate that rcAAV levels be minimized in clinical AAV preparations.

The generation of rcAAV particles during the rAAV vector production process is a recognized challenge.[7,8] The predominant method to produce rAAVs involves triple transfection of HEK293 cells, compromising a helper plasmid (Rep/Cap plasmid) that provides the Cap and Rep proteins in *trans*,[9] an adenovirus (Ad) helper plasmid (pHelper) that delivers Ad helper genes, and a *cis* plasmid delivering the gene of interest flanked by ITRs[10] (AAV genome/vector plasmid).[11] In contrast to wild-type AAV, which carries both rep and cap genes within its genome, the rAAV genome contains only the therapeutic transgene cassette flanked by ITRs; the *rep* and *cap* genes are supplied in *trans* during vector production and are therefore absent from the rAAV genome. This distinction underlies our detection strategy, as qPCR assays targeting the rep gene will specifically detect rcAAV (or wtAAV) but not rAAV genomes. Co-expression of *rep*, *cap*, and vector genes in a single cell leads to unavoidable homologous/non-homologous recombination

Received 19 May 2025; accepted 28 August 2025;
https://doi.org/10.1016/j.omtm.2025.101584.

[9]These authors contributed equally

Correspondence: Chen Ling, State Key Laboratory of Genetic Engineering and Engineering Research Center of Gene Technology (Ministry of Education), School of Life Sciences, Zhongshan Hospital, Fudan University, Shanghai 200438, China.
E-mail: lingchenchina@fudan.edu.cn
Correspondence: Liqing Zhu, Department of Clinical Laboratory, Peking University Cancer Hospital & Institute, Beijing 100142, China.
E-mail: zhuliqing@bjmu.edu.cn
Correspondence: Bicui Zhan, Department of Clinical Laboratory, Hangzhou TCM Hospital Affiliated to Zhejiang Chinese Medical University, Hangzhou, Zhejiang 310007, China.
E-mail: 23419645@qq.com

between AAV DNAs, generating rcAAVs.[12,13] Theoretically, minimizing recombination can reduce the production of rcAAVs.[7] Given the limitations of current detection methods, the precise level of rcAAV contamination may be underestimated, but the theoretical possibility of their generation remains a critical concern. Indeed, several approaches have been proposed, such as replacing the p5 promoter region in the rAAV genome,[14] constructing a new AAV packaging plasmid to carry separate *rep* and *cap* expression cassettes in opposite transcriptional orientations,[15] or expressing different genes in separate subcellular compartments to prevent their interaction. However, these approaches, while promising, often require significant changes to established manufacturing processes. Nevertheless, they are being actively explored and adopted by industry to further reduce rcAAV levels.

Monitoring rcAAV content in both the production and final products of rAAV samples becomes a critical factor. This importance is further emphasized by various regulatory agencies, including the US FDA,[16] the EMA,[17,18] and the National Medical Products Administration.[19,20] To establish safety standards, the industry has widely adopted a target of limiting rcAAV content to less than 1 infectious unit (IU) per 1E8 vector genomes (vg), or even less than 1 IU per 3E10 vg, based on recommendations from published studies.[21,22] To ensure reliable quantification of rcAAV, the cell culture-based amplification method is considered the gold standard. This method involves infecting HEK293 cells with rAAV particles, with or without a positive control, followed by three rounds of continuous passaging with the help of recombinant Ad (rAd)5. During three rounds of rcAAV genome replication, the relatively low initial quantification in the sample is amplified. After each round, infected cells are harvested for genomic DNA extraction, which is then analyzed for AAV *rep* gene detection via quantitative real-time PCR (qPCR), as shown in Figure 1A.[7,23] However, despite its status as the gold standard, this assay is not well documented in scientific literature, with a limited description of a prototype assay provided in Allen et al.[3] The lack of a detailed, published protocol makes replication of this assay difficult and inconsistent, which should be noted. This method can yield false-negative results, as observed in earlier researches. If the rcAAV concentration in a sample is too low or if the serotype is less efficient at infecting the HEK293 cells, the rcAAV may not be detected in serial cell cultures, even when the amount exceeds the commonly accepted threshold of 1 IU of rcAAV per 1E+8 vg rAAV.

In this study, we found that high-titer rAAV competitively inhibits rcAAV replication in host cells, causing false-negative results. To enhance rcAAV detection sensitivity and precision, we engineered HEK293 cell lines to overexpress SpCas9 and used rAd5 vectors, including rAd5-gNC as a negative control, to deliver single-guide RNA (sgRNA) targeting loci in the rAAV genomes, constructing a CRISPR system that cleaves the rAAV genome during detection. This approach efficiently reduces background interference and improves assay accuracy and sensitivity.

RESULTS

Interference of rAAV in rcAAV detection

A qPCR analysis targeting the rep gene during the rAAV2-gfp preparation indicated that rcAAV genome was below the limit of detection of our assay, which was determined to be less than 1 IU per 3E10 vg, after three rounds of amplification. Meanwhile, we observed no increase in copies of ITR after three rounds of replication, indicating that the replication of rAAV2-gfp genomes in HEK293 cells may have reached the upper limit or its assay saturation level (Figure 1B). This indicated that a high copy number of rAAV genomes was present, a necessary condition for our hypothesis. Based on these findings, we hypothesized that if rcAAVs are present in the sample, the replication of a large quantity of rAAV genomes might interfere with their replication, which leads to false-negative results of rcAAV detection. To test this hypothesis, 1×10^{11} vg of rAAV2-*gfp* or an equal volume of PBS control was mixed with 2×10^{2} vg or 1×10^{3} vg of vsub201, a well-characterized replication-competent AAV2 mimic with a wild-type AAV2 genome, which is commonly used as a positive control for rcAAV detection. The mixtures were subjected to a cell culture-based rcAAV detection assay. As shown in Figures 1C and 2, 1×10^{2} vg of vsub201 failed to replicate sufficiently to detect the *rep* gene, regardless of the presence or absence of rAAV2-*gfp*, indicating a limitation of the assay. In contrast, 1×10^{3} vg of vsub201 exhibited an increase in *rep* gene copy number after three rounds of replication in the absence of rAAV2-*gfp*. Notably, the same amount of vsub201 failed to replicate in the presence of 1×10^{11} vg of rAAV2-*gfp* vectors (Figure 1C). In contrast, 1×10^{11} vg of rAAV2-*gfp* genome increased efficiently and reached upper limit post three rounds of replication, as indicated by the ITR primers (Figure 1D). To further validate our hypothesis and ensure that it is the rAAV component that inhibits the replication of the rcAAV genome, 1×10^{5} vg, 1×10^{7} vg, or 1×10^{9} vg of rAAV2-*gfp* was mixed with 1×10^{3} vg of vsub201. The mixtures were subjected to a cell culture-based rcAAV detection assay. As shown in Figure 1E, vsub201 replicated in the presence of 1×10^{5} vg or 1×10^{7} vg of rAAV2-*gfp*. However, vsub201 failed to replicate in the presence of 1×10^{9} vg of rAAV2-*gfp*. These observations suggested that interference from rAAV2-*gfp* leads to false-negative results of rcAAV detection.

Establishment of a SpCas9-HEK293 cell line for rcAAV detection

It has been hypothesized that CRISPR-mediated cleavage of the rAAV genome in HEK293 cells would mitigate the impact of rAAV on rcAAV replication, thereby enhancing the sensitivity of rcAAV detection. To test this hypothesis, lentiviral transduction followed by antibiotic selection was used to generate a stable HEK293 cell line overexpressing flag-tagged SpCas9, hereafter referred to as SpCas9-HEK293. As shown in Figure 2A, stable expression of SpCas9 was confirmed by western blot (WB) analysis across multiple passages. Additionally, immunofluorescence analysis indicated that 87.44% (standard deviation [SD] = 11.94%) of the cells exhibited SpCas9 overexpression (Figure 2B). The red fluorescence of SpCas9 overlaps with the blue fluorescence of DAPI staining, indicating that the SpCas9 protein, containing a nuclear localization signal, is predominantly localized in the nucleus.

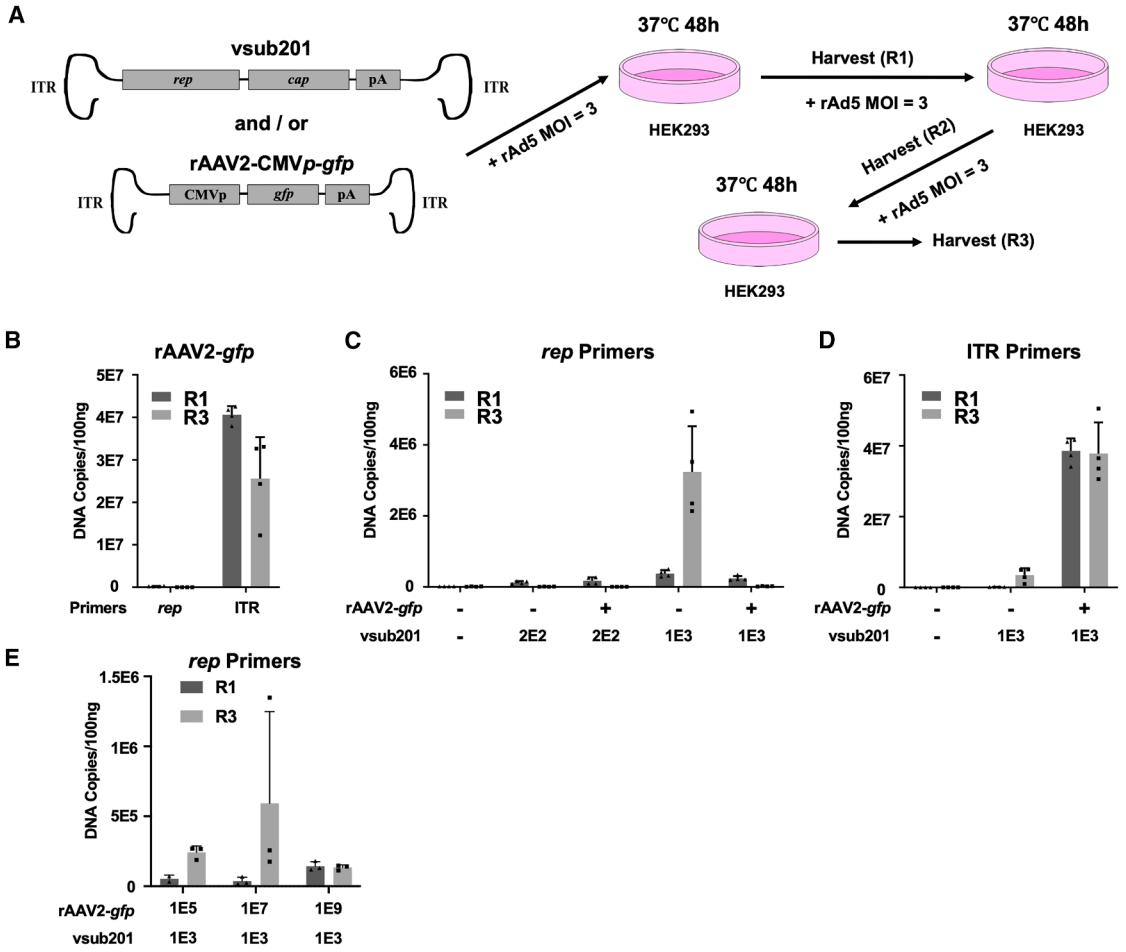

Figure 1. Schematic of traditional rcAAV detection and its limitations

(A) Schematic of cell culture method for rcAAV detection. The rcAAV detection method involves allowing rAAV samples to replicate in HEK293 cells for three rounds, facilitated by rAd5. vsub201 acts as a mimic of wild-type AAV2. Following replication, genomic DNA is extracted from the cells, and the copy number of the *rep* gene (rcAAV genome) is quantified. (B) Replication of rcAAV in HEK293 cells. rAAV2-CMV*p-gfp* samples at 1E11 vg were tested for rcAAV replication as described in the materials and methods. After three rounds of replication, qPCR was performed to quantify the copies of the rep and ITR sequences. Graph bars represent means ± SD of $n = 4$ experiments. (C and D) Effect of rAAV on replication of low and high titer vsub201. vsub201 samples at 2E2 vg (low) or 1E3 vg (high) were incubated with or without 1E11 vg of rAAV2-CMV*p-gfp*. rcAAV replication was assessed according to the protocol in the materials and methods. After three rounds of replication, qPCR was conducted to quantify the copies of the (C) rep and (D) ITR sequences. Graph bars represent means ± SD of $n = 4$ experiments. (E)Effect of low and high titer rAAV on replication of vsub201. vsub201 samples at 1E3 vg were incubated with 1E5/1E7/1E9 vg of rAAV2-CMVp-*gfp*. rcAAV replication was assessed according to the protocol in the materials and methods. After three rounds of replication, qPCR was conducted to quantify the copies of the rep sequences. Graph bars represent means ± SD of $n = 3$ experiments.

To evaluate the cutting efficiency of our SpCas9-HEK293 cell line, we designed sgRNAs targeting the *itih5*, *cxcr4*, *dnase2*, *and dnase1l1* loci. The sgRNA delivery plasmids were transfected into the cell lines, and the indel efficiency was 35.8%, 34.1%, 11.7%, and 31.6%, respectively (Figure 2C). These results established the SpCas9-HEK293 cell line as a reliable CRISPR-based genome editing platform.

The SpCas9-HEK293 cell line satisfies the fundamental requirements for rcAAV detection

The transduction efficiency of rAAV and rAd5 vectors in the SpCas9-HEK293 cell line was assessed next. No significant differences in fluorescence intensity were observed between HEK293 and SpCas9-HEK293 cells 72 h post transduction with rAAV2-*gfp* (multiplicity of infection [MOI] 1E5 vg/cell), rAAV6-*gfp* (MOI 1E5 vg/cell), or rAd5-*mCherry* (MOI 50 vg/cell) vectors (Figure 3A). Importantly, the similar transduction efficiency of rAd5 observed in SpCas9-HEK293 and HEK293 cells ensures that differences in rAd5 infection do not confound rcAAV replication or detection in our system. In accordance with previous studies, a lower transduction efficiency of rAAV6 compared to rAAV2 was observed.[25] Furthermore, the genome of vsub201, a widely used mimic of wild-type AAV2, replicated efficiently in both HEK293 and SpCas9-HEK293 cell lines in the presence of rAd5-*mCherry* (Figures 3B and S1). Additionally, the packaging efficiencies of

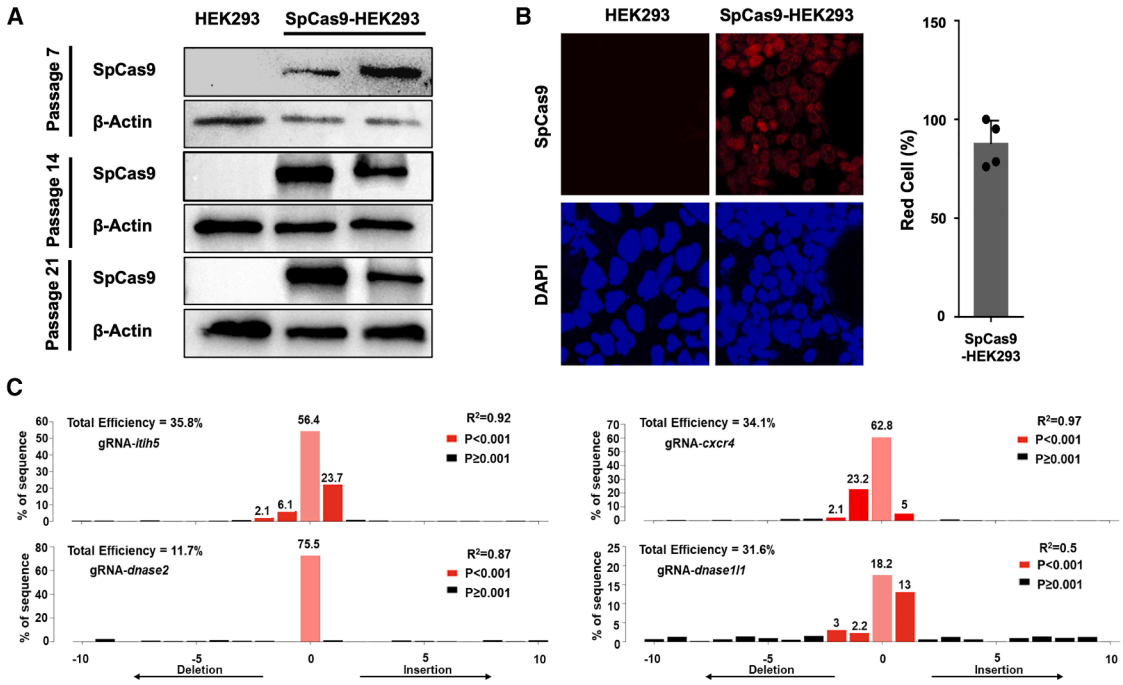

Figure 2. Characterization of HEK293 cell line overexpressing SpCas9

(A) Western blot analysis of SpCas9 expression in SpCas9-HEK293 cells after passaging. SpCas9-HEK293 clones were obtained, and cell samples from the 7th, 14th, and 21st generations were collected for analysis. Cell lysates (200 μg per lane) were loaded onto a gel, and western blotting was performed using an anti-SpCas9 antibody to detect SpCas9 expression. (B) Immunofluorescence analysis of SpCas9 expression in SpCas9-HEK293 cells by confocal microscopy. Confocal microscopy images of SpCas9 expression in SpCas9-HEK293 cells at passage 21 were captured at 160× magnification. The red fluorescence indicates FLAG-tagged SpCas9, detected with a rabbit anti-FLAG antibody and a Cy3-conjugated secondary antibody. Nuclei were stained with DAPI, appearing blue. The percentage of red cells was quantified using ImageJ. Graph bars represent means ± SD of $n = 4$ experiments. (C) Indel spectrum of target gene edited by SpCas9 in HEK293 cells. gRNAs targeting endogenous genes *itih5*, *danse2*, *cxcr4*, and *dnase1l1* were transfected into SpCas9-HEK293 cells. After 48 h, genomic DNA was extracted, and PCR amplification of the target gene fragments was performed. Sequencing results analyzed by TIDE[24] confirmed cleavage of the target sequences, as guided by the respective gRNAs.

rAAV vectors in both HEK293 and SpCas9-HEK293 cells were compared. The production of various rAAV vectors, carrying either the *gfp* or *fluc* gene, was assessed following triple transfection of both cell lines. No significant difference in vector titers was observed between the two cell lines (Figure 3C). These results suggested that the SpCas9-HEK293 cell line can serve as a suitable platform for cell culture-based amplification methods in rcAAV detection.

Transfection of SpCas9-HEK293 cell line with sgRNA plasmids efficiently cleaves rAAV DNA in plasmids

Aiming to test the feasibility of sgRNA-mediated cleavage in this context, SpCas9-HEK293 cells were co-transfected with an Amp-resistant plasmid containing the rAAV genome and a KaN-resistant plasmid delivering the corresponding sgRNA (Figure 4A). A series of computationally predicted sgRNAs targeting loci such as the promoter, intron, *gfp* cassette, 3′ UTR, 5′ UTR, and polyA site were employed for screening. Several sgRNAs significantly reduced the fluorescence expression driven by the rAAV genome plasmid, indicating efficient cleavage of the rAAV genomic DNA (Figure 4B). The polyA signal sequence targeted in this study is a feature of the rAAV genome downstream of the transgene cassette. It is absent in the wild-type AAV (including rcAAV) genome, ensuring that the CRISPR-Cas9-mediated cleavage selectively eliminates rAAV genomes while leaving rcAAV genomes unaffected. Given the common presence of polyA signal sequences across multiple rAAV genome plasmids shown in the table below Figure 4B, subsequent experiments focused on sgRNAs targeting this region (gpA1 and gpA2).

The rAAV genome plasmid (Amp-resistant) and the sgRNA-delivering plasmid (KaN-resistant) were co-transfected into both HEK293 and SpCas9-HEK293 cells (Figure 4C). No significant difference in fluorescence was observed between the negative control and gpA groups in HEK293 cells. However, GFP expression was significantly reduced in SpCas9-HEK293 cells, showing a 10.15-fold decrease in the presence of gpA1 ($p = 0.0029$) and a 6.43-fold decrease in the presence of gpA2 ($p = 0.0187$). To quantify cleavage efficiency, Hirt DNA was extracted 72 h post transfection and used to transform competent DH5α bacterial cells. Colonies arising from the intact rAAV genome plasmid were selected on Amp-resistant LB plates. An approximately 4-fold reduction in colony formation was observed in samples co-transfected with either gpA1 or gpA2, confirming cleavage of the rAAV genome plasmid.

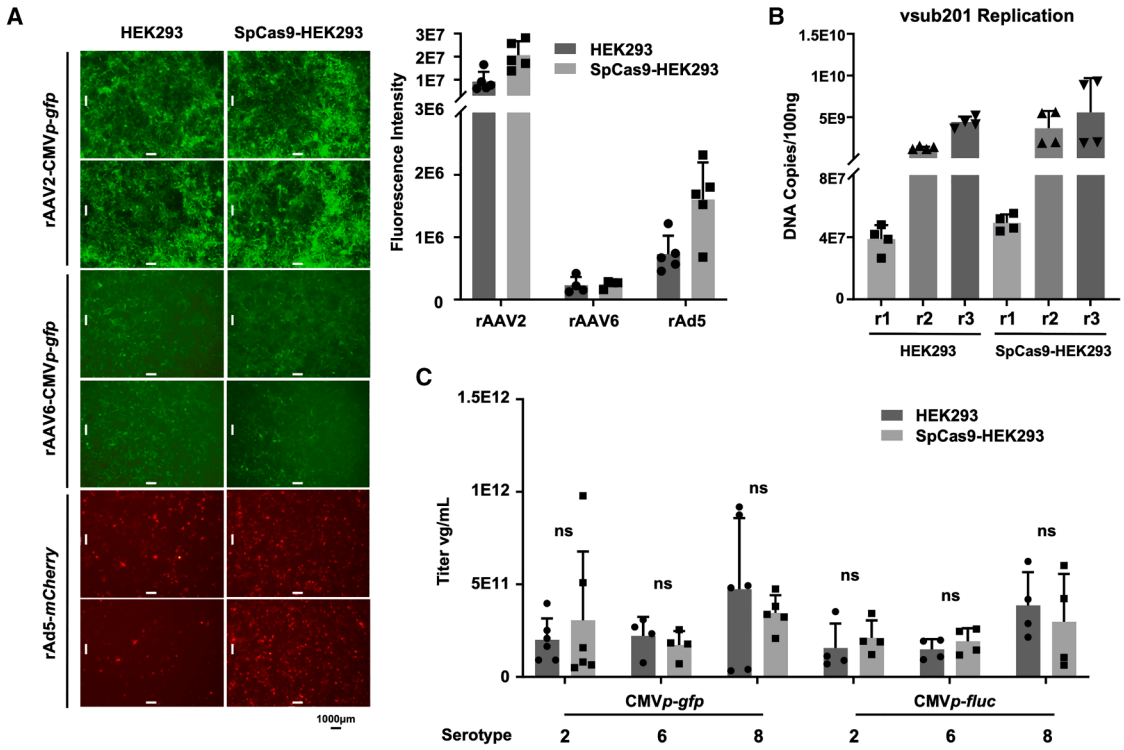

Figure 3. SpCas9-HEK293 cell line as an alternative to HEK293 for rcAAV quantification

(A) Comparison of rAAV and rAd transduction efficiency in HEK293 and SpCas9-HEK293 cells. HEK293 and SpCas9-HEK293 cells were transduced with rAAV2-CMV*p-gfp*, rAAV6-CMV*p-gfp*, and rAd5-*mCherry* at an MOI of 1E5. Fluorescence was observed 72 h post transduction using a fluorescence microscope, as shown in the image on the left. Fluorescence intensity was quantified with ImageJ. Graph bars represent means ± SD of $n = 5$ experiments. (B) vsub201 replicates efficiently in SpCas9-HEK293 cells with rAd5 assistance. HEK293 and SpCas9-HEK293 cells (2E6 cells/well) were co-transduced with rAd5 at an MOI of 30 and vsub201 at an MOI of 1E5. rcAAV replication was assessed according to the protocol outlined in the materials and methods. Genomic DNA was extracted from the cells after each round of replication, and then qPCR was performed to quantify the copies of ITR sequences. Graph bars represent means ± SD of $n = 4$ experiments. (C) SpCas9-HEK293 cells do not affect rAAV packaging efficiency. rAAV serotypes 2, 6, and 8 (*gfp/fluc*) were packaged. Physical titers, measured as genome titer by qPCR, were analyzed following the protocol in the materials and methods. Graph bars represent means ± SD of $n \geq 4$ experiments.

Enhancing rcAAV detection sensitivity using SpCas9-HEK293 cells with rAd5-sgRNA vectors

The rAd5-gpA1 vectors were generated using the AdEasy system. SpCas9-HEK293 cells were co-infected with rAd5-gpA1 and double-stranded rAAV2-*gfp* vectors (Figure 5A). The rAd5-gNC vector, which delivers an unrelated sgRNA, was used as a negative control. The results showed that rAd5-gNC promoted rAAV-mediated transgene expression, which was expected because Ad is reported to act as an AAV helper virus.[26] However, fluorescence was significantly reduced in the presence of rAd5-gpA1 (Figure 5B), suggesting that the rAAV2-*gfp* genome was cleaved by SpCas9 in conjunction with gpA1. Subsequently, total cellular DNA was extracted for *gfp* DNA quantification. Fewer copies of *gfp* DNA were detected in the rAd5-gpA1 group, with a reduction percentage of 70.95% (SD = 9.13%) compared to the negative control group. This further confirmed the successful cleavage of the rAAV genome plasmid (Figure 5C).

Finally, the SpCas9-HEK293-based amplification system was evaluated for rcAAV detection. When rAAV genomes were cleaved by gpA1, the number of rcAAV genomes detected increased by three times in replication round 1 and five times in replication round 3 (Figure 5D). Additionally, vsub201 (2E3 vg) was introduced into SpCas9-HEK293 cells, with or without 1E11 vg of rAAV2-*gfp*, and applied to our CRISPR-based rcAAV detection method (Figure 5E). While the traditional method failed to detect rcAAV at this low concentration in the presence of rAAV2-gfp (as shown in Figure 1C), vsub201 could be detected at levels as low as 3E2 vg with our CRISPR-based system, despite interference from rAAV-*gfp*. Our optimized method outperformed the traditional approach in detection limit and sensitivity, with less false-negative results.

DISCUSSION

It has been proposed that high concentrations of rAAV in a sample inhibit rcAAV replication, leading to false-negative results. Simply reducing the rAAV load will not resolve this issue, as it would proportionally dilute the rcAAV. Indeed, when the rcAAV concentration is reduced below a critical threshold (e.g., 2×10^2 vg, as shown in

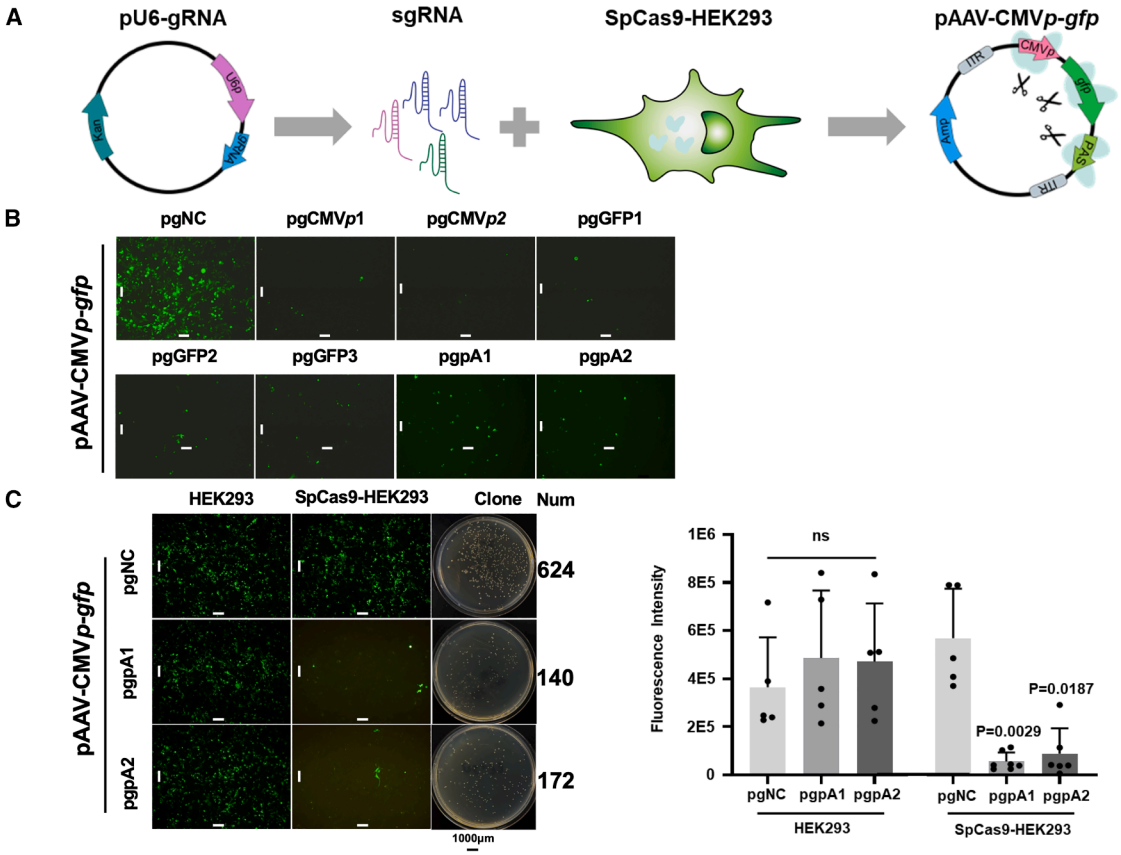

Figure 4. CRISPR-based rcAAV quantification method and its validation

(A) Schematic of the CRISPR-based gRNA cleavage evaluation method for AAV genome. To assess the effectiveness of selected gRNAs in cleaving the AAV genome, HEK293 cells engineered to overexpress SpCas9 were co-transfected with the pAAV-CMV*p-gfp* plasmid and a U6 promoter-driven plasmid delivering a gRNA that targets multiple sites in the rAAV genome. (B) Screening of gRNAs for cleavage of the pAAV-CMV*p-gfp* plasmid. Multiple gRNA sequences predicted by DeepHF to target specific regions were selected and integrated into the U6 promoter-driven delivery plasmids. SpCas9-HEK293 cells were transfected with these plasmids separately, along with 2 μg of pdsAAV-CMV*p-gfp* in all groups. After 72 h, fluorescence was observed. The table below provides a summary of the polyA signal types commonly present in existing rAAV genome plasmids, along with the representative plasmids associated with each signal type. (C) Verification of gRNA delivery plasmids for cutting the polyA site in the pdsAAV-CMV*p-gfp* plasmid. Two gRNA sequences, gpA1 and gpA2, predicted to target the polyA site, were integrated into the delivery plasmids. SpCas9-HEK293 and HEK293 cells were transfected with these plasmids and 2 μg of pdsAAV-CMVp-gfp. After 72 h, fluorescence was observed, and Hirt DNA was extracted and used to transform *E. coli*. Upper: the fluorescence image and transformation of Hirt DNA into *E. coli* on an ampicillin-resistant plate. Lower: fluorescence quantification using ImageJ. Graph bars represent means ± SD of $n = 5$ experiments.

Figure 1C), it becomes undetectable after three rounds of replication. Digital droplet PCR (ddPCR) may enhance rcAAV detection, offering higher sensitivity and accuracy by partitioning the sample into thousands of individual reactions. This approach enables precise quantification of low-copy DNA, making ddPCR more effective for detecting rcAAV at low concentrations. Additionally, primer selection in qPCR plays a crucial role in detection efficiency. Reliable primers should target the distal 10 nucleotides of the D sequence in the left ITR and the 5′ end of the *rep* gene. Insufficient amplification of the *cap* gene can lead to false-negative results, as it may be absent in rcAAVs.[8]

In this study, a novel method for detecting rcAAV contamination in rAAV samples using the CRISPR system has been introduced. Conventional methods fail to detect 3×10^2 vg of rcAAV in 1×10^{11} vg rAAV samples, whereas our CRISPR-based approach can detect rcAAV at such low levels. This method utilizes rAd5 vectors to deliver guide RNAs (gRNAs) targeting the rAAV genome, along with overexpression of SpCas9 in HEK293 cells. Over three rounds of amplification, SpCas9, guided by the gRNAs, cleaves the rAAV genome. Theoretically, this strategy should eliminate interference from rAAV genomes, thereby maximizing the amplification of rcAAV genomes. However, at present, our CRISPR-based method does not achieve complete cleavage of rAAV genomes. Further optimization is required to enhance the efficiency of rAAV genome cleavage and improve the sensitivity of rcAAV genome detection.

The detection of rcAAV in non-AAV2 samples poses a significant challenge due to considerable variation in infection efficiency across

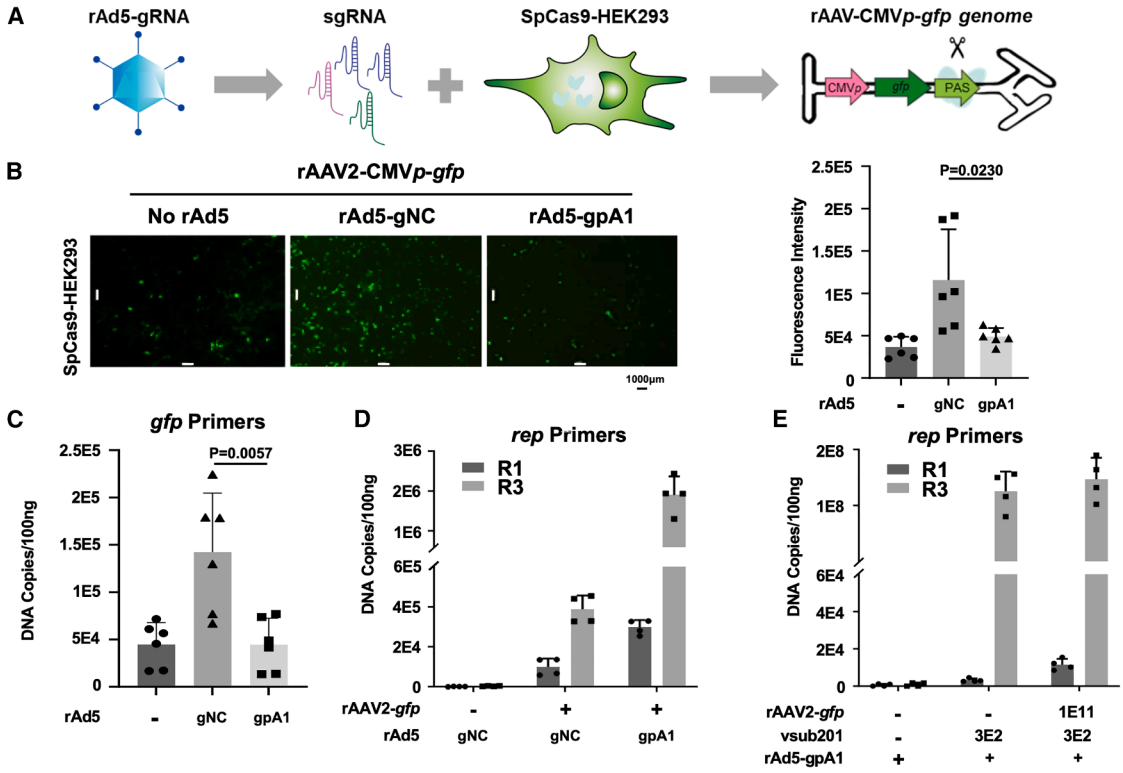

Figure 5. Superior sensitivity and detection limits of CRISPR-based rcAAV quantification compared to traditional method

(A) Schematic of the CRISPR-based rcAAV detection method. In our CRISPR-based rcAAV detection method, HEK293 cells engineered to overexpress SpCas9 were co-transfected with the rAAV sample and rAd5, which delivered the gRNA targeting the polyA site in the rAAV genome. (B) Fluorescence imaging of rAAV2-CMV*p-gfp* genome cutting in SpCas9-HEK293 cells SpCas9-HEK293 cells were transduced with rAAV2-CMV*p-gfp* (MOI = 2E4) with or without co-infection of rAd5-gNC or rAd5-gpA1 (MOI = 3). After 72 h, fluorescence images were captured (left), and fluorescence intensity was quantified (middle). Graph bars represent means ± SD of *n* = 6 experiments. (C) qPCR analysis of rAAV2-CMV*p-gfp* cleavage in SpCas9-HEK293 cells after fluorescence images was captured, genomic DNA was extracted from the cells, and qPCR was performed to quantify the copies of *gfp* sequences. Graph bars represent means ± SD of *n* = 6 experiments. (D) gpA1-mediated polyA site cutting enhances rcAAV detection sensitivity. 1E11 vg of rAAV2-*gfp* was co-administered with either rAd5-*mCherry* or rAd5-gpA1 for rcAAV detection. Genomic DNA was extracted after the third round of replication, and qPCR was performed to quantify the copies of *rep* sequences. Graph bars represent means ± SD of *n* = 4 experiments. (E) CRISPR-based rcAAV detection method identifies 3E2 vg of rcAAV under high rAAV interference. vsub201 samples at 3E2 vg were incubated with or without 1E11 vg of rAAV2-*gfp*. rcAAV replication was assessed using our CRISPR-based rcAAV detection method. After three rounds of replication, qPCR was performed to quantify the rep sequence copies. Graph bars represent means ± SD of *n* = 4 experiments.

different serotypes. Certain serotypes, such as 4, 5, and 7, exhibit much lower infection efficiency in the HEK293 cell line compared to serotype 2, leading to an underestimation of rcAAV content.[24] To address this issue, further engineering of our SpCas9-HEK293 cell line to overexpress specific receptors, such as AAVR and GPR108, may enhance infection efficiency and enable more accurate detection of rcAAV content.[27]

In addition to the aforementioned, our CRISPR-based detection strategy was designed to target conserved sequences within the rAAV genome, such as the polyA region, which are generally retained across vectors produced using different packaging systems, including triple plasmid transfection, baculovirus/Sf9, and herpes simplex virus-based methods. This design allows the method to be broadly applicable to rAAV samples from diverse manufacturing platforms. Nevertheless, differences in vector genome configuration, helper virus components, capsid serotypes, and particle-to-infectivity ratios among these production systems may influence transduction efficiency in the SpCas9-HEK293-based assay, thereby impacting rcAAV detection sensitivity. In such cases, assay performance could be further optimized by incorporating capsid-specific receptor overexpression (e.g., AAVR, GPR108) into the SpCas9-HEK293 cell line or by adapting the method to alternative permissive cell types for initial amplification.

Additionally, detecting rAAV samples expressing protein toxins is particularly challenging, as these toxins can induce cell death when overexpressed, rendering cell-based replication assays ineffective.[28,29] Strategies that cleave the rAAV genome could reduce protein toxin expression, thereby enabling more reliable detection of rcAAV content in such samples. It is also notable that SpCas9-HEK293 cell line may not be suitable for detecting rAAV samples

carrying sgRNA expression cassettes. In such cases, the expressed gs could direct Cas9 to cleave endogenous genomic loci, potentially impairing cell viability and affecting the accuracy of rcAAV detection.

In conclusion, the sensitivity of our optimized CRISPR-based rcAAV detection method makes it applicable to a wide range of rAAV samples, with significant potential for further development to enhance patient safety by minimizing rcAAV contamination, thereby aligning with the rigorous standards required for human clinical trials.

MATERIALS AND METHODS

Generation of rAAV and rAd

The rAAV vectors used in this study were produced by triple transfection method of HEK293 cells (CRL-1573, ATCC, USA), which were cultured in DMEM (319-005-CL, WISENT, China) supplemented with 10% fetal bovine serum (FBS) (098-150, WISENT, China) and 1% penicillin-streptomycin (086-550, WISENT, China) as previously described.[30] The rAAV vectors were harvested 72 h post transfection, and their physical titers were determined using an optimized method previously published by our group.[31]

The rAd containing gRNAs were generated using the AdEasy system, following the manufacturer's recommended procedures.[32] The sgRNAs targeted the polyA site downstream of the *gfp* expression cassette in the rAAV vector genomes, as follows:

gNC: CAGGGTCAAGGAAGGCACGG

gpA1: CCCCGTGCCTTCCTTGACCC

gpA2: GCAACTAGAAGGCACAGTCG

To assess the potential off-target effects of the designed gRNAs, the online tool CCTOP (CRISPR-Cas9 Target Online Predictor)[33] was utilized for *in silico* prediction. The tool predicted that none of the selected gRNAs exhibited significant off-target effects under the specified experimental conditions.

The rAd5-*mCherry* was generously provided by Tongji University. All rAds were amplified and purified using the Vivapure AdenoPACK 20 RT (VS-AVPQ022, Sartorius, Germany) according to the manufacturer's guidelines.

HEK293 overexpressing SpCas9 construction

The coding sequence of SpCas9 was cloned into the lentiviral pLV vector using the ClonExpress Ultra One Step Cloning Kit V2 (C116, Vazyme, China), with BamH I and EcoR I restriction sites. The vectors were generated via transient three-plasmid transfection, as described previously.[34] HEK293 cells were seeded in 6-well plates 1 day prior, and when the confluence reached approximately 60%, 2 mL of Lentivirus-SpCas9 was added along with polybrene to a final concentration of 10 μg/mL. After 6 h of infection, the medium was replaced with DMEM containing 10% FBS. The selection was performed using 2 μg/mL puromycin for 14 days, and SpCas9-HEK293 clones were obtained. Stable expression of SpCas9 was verified by WB and immunofluorescence analyses.

Detection of rcAAV

rcAAV vectors were sequentially amplified and detected as previously described.[3] The vsub201 vector, which mimics wild-type AAV2 and harbors a replication-competent AAV2 genome, was employed as a positive control in our rcAAV detection assays. It contains the full set of *rep* and *cap* genes required for autonomous replication in the presence of a helper Ad, serving as a reliable standard for rcAAV quantification. In the first amplification, HEK293 cells were seeded overnight in 6-well plates to reach a density of 1E6 cells per well. rAd5-*mCherry* or rAd5-gRNAs were added to each well at a MOI of 3, and rAAV vectors were introduced at genome particle concentrations ranging from 5E10 to 1E11. After 48 h of infection, cells were collected and subjected to three cycles of freeze/thaw, followed by heating at 56°C for 1 h to deactivate rAd5. For the second and third amplifications, HEK293 cells were infected with rAd5 and the freeze/thaw lysates from the previous step for an additional 48 h. Cells were then pelleted, washed with PBS, and genomic DNA was extracted using the Trelief Hi-Pure Animal Genomic DNA Kit (TSP202-200, Tsingke, China). To detect the *rep* genes (essential for rcAAV replication), qPCR was performed using the Tsingke 2× qPCR SYBR Green I mix (TSE201, Tsingke, China), following the manufacturer's protocols. The primers used for amplification of the *rep* gene were as follows:

Forward primer: CTCCATCACTAGGGGTTCC

Reverse primer: GGCAGATGCCCGTCAAGGT

Vector transduction and detection by fluorescence microscopy

HEK293 cells were transduced with rAAV vectors and/or rAd5 at the appropriate MOI in 96-well or 6-well plates, depending on the experimental setup. The vectors were added to a serum-free culture medium, and cells were incubated at 37°C for 2 h. After incubation, the medium was replaced with fresh DMEM containing 10% FBS, and the cells were cultured for an additional 48 h to allow for GFP and/or mCherry expression. Fluorescence was then observed and captured using a fluorescence microscope to detect rAAV and/or rAd5 transduction.

Statistical analyses

Data are presented as the group mean ± SD. Statistical analysis was performed using Prism v.9.0 (GraphPad Software, USA). For comparisons between the two groups, a Student's t test was used. For multiple group comparisons, one-way ANOVA followed by Tukey's post hoc test was applied. Normality was assessed using the Shapiro-Wilk test, and statistical significance was defined as p value.

DATA AND CODE AVAILABILITY

The data supporting the findings of this study are available within the article and its supplementary materials. All of the data that support the findings of this study are available from the corresponding author upon reasonable request. The datasets used and/or

analyzed during the current study are available from the corresponding author upon reasonable request. All unique/stable reagents generated in this study are available from the lead contact with a completed materials transfer agreement.

ACKNOWLEDGMENTS

We sincerely thank Professor Yongming Wang from the School of Life Sciences, Fudan University, for kindly providing the SpCas9 plasmid and for his generous support throughout this study. We are grateful to Dr. Chenghui Yu and Dr. Yao Wang from the same institute for their valuable technical assistance. Special thanks also go to Mr. Huawei Xu for his dedicated help during the experimental procedures. This work was sponsored by grants from National Key R&D Program of China #2023YFC3403301 (to C.L.), the National Natural Science Foundation of China #82272784 (to L.Z.), Wenzhou Major Scientific and Technological Innovation Project #ZY2022001 (to L.Z.), and the agricultural and social development project of Hangzhou #20241029Y059 (to B.Z.).

DECLARATION OF GENERATIVE AI AND AI-ASSISTED TECHNOLOGIES IN THE WRITING PROCESS

During the preparation of this work, the authors used Chat Generative Pre-trained Transformer 3.5 in order to improve readability. After using this tool, the authors reviewed and edited the content as needed and took full responsibility for the content of the publication.

AUTHOR CONTRIBUTIONS

B.Z. and L.Z. established the overarching research goals and objectives. K.Y., M.Y., and C.L. designed the experimental methodology. M.Y., S.S., X.Z., and Q.Z. conducted the experiments. S.S., Q.Z., F.H., and K.W. performed data analysis. Q.K., L.W., and X.G. produced and purified the viral vectors. X.G., M.Y. and C.L. wrote the manuscript. B. Z., L.Z. and C.L. supervised the planning and execution of the research activities. All authors reviewed and approved the final manuscript.

DECLARATION OF INTERESTS

X.Z. is an employee of Zhejiang Hengyu Biological Technology Co., Ltd., a company that provides high-standard and comprehensive biological safety testing solutions to innovative pharmaceutical enterprises globally. X.Z. also holds equity stakes in the company.

SUPPLEMENTAL INFORMATION

Supplemental information can be found online at https://doi.org/10.1016/j.omtm.2025.101584.

REFERENCES

1. Wang, J.H., Gessler, D.J., Zhan, W., Gallagher, T.L., and Gao, G. (2024). Adeno-associated virus as a delivery vector for gene therapy of human diseases. Signal Transduct. Target. Ther. *9*, 78. https://doi.org/10.1038/s41392-024-01780-w.

2. Qiu, Y., Liu, X., Sun, Y., Li, S., Wei, Y., Tian, C., and Ding, Q. (2021). In Situ Saturating Mutagenesis Screening Identifies a Functional Genomic Locus that Regulates Ucp1 Expression. Phenomics *1*, 15–21. https://doi.org/10.1007/s43657-020-00006-7.

3. Allen, J.M., Debelak, D.J., Reynolds, T.C., and Miller, A.D. (1997). Identification and elimination of replication-competent adeno-associated virus (AAV) that can arise by nonhomologous recombination during AAV vector production. J. Virol. *71*, 6816–6822. https://doi.org/10.1128/jvi.71.9.6816-6822.1997.

4. Wright, J.F. (2014). Product-Related Impurities in Clinical-Grade Recombinant AAV Vectors: Characterization and Risk Assessment. Biomedicines *2*, 80–97. https://doi.org/10.3390/biomedicines2010080.

5. Pien, G.C., Basner-Tschakarjan, E., Hui, D.J., Mentlik, A.N., Finn, J.D., Hasbrouck, N.C., Zhou, S., Murphy, S.L., Maus, M.V., Mingozzi, F., et al. (2009). Capsid antigen presentation flags human hepatocytes for destruction after transduction by adeno-associated viral vectors. J. Clin. Investig. *119*, 1688–1695. https://doi.org/10.1172/jci36891.

6. Mingozzi, F., Maus, M.V., Hui, D.J., Sabatino, D.E., Murphy, S.L., Rasko, J.E.J., Ragni, M.V., Manno, C.S., Sommer, J., Jiang, H., et al. (2007). CD8(+) T-cell responses to adeno-associated virus capsid in humans. Nat. Med. *13*, 419–422. https://doi.org/10.1038/nm1549.

7. Dong, B., Moore, A.R., Dai, J., Roberts, S., Chu, K., Kapranov, P., Moss, B., and Xiao, W. (2013). A concept of eliminating nonhomologous recombination for scalable and safe AAV vector generation for human gene therapy. Nucleic Acids Res. *41*, 6609–6617. https://doi.org/10.1093/nar/gkt404.

8. Wang, X.S., Khuntirat, B., Qing, K., Ponnazhagan, S., Kube, D.M., Zhou, S., Dwarki, V.J., and Srivastava, A. (1998). Characterization of wild-type adeno-associated virus type 2-like particles generated during recombinant viral vector production and strategies for their elimination. J. Virol. *72*, 5472–5480. https://doi.org/10.1128/jvi.72.7.5472-5480.1998.

9. Phillips, M.I. (1997). Antisense inhibition and adeno-associated viral vector delivery for reducing hypertension. Hypertension *29*, 177–187. https://doi.org/10.1161/01.hyp.29.1.177.

10. Savy, A., Dickx, Y., Nauwynck, L., Bonnin, D., Merten, O.W., and Galibert, L. (2017). Impact of Inverted Terminal Repeat Integrity on rAAV8 Production Using the Baculovirus/Sf9 Cells System. Hum. Gene Ther. Methods *28*, 277–289. https://doi.org/10.1089/hgtb.2016.133.

11. Liu, H., Zhang, Y., Yip, M., Ren, L., Liang, J., Chen, X., Liu, N., Du, A., Wang, J., Chang, H., et al. (2024). Producing high-quantity and high-quality recombinant adeno-associated virus by low-cis triple transfection. Mol. Ther. Methods Clin. Dev. *32*, 101230. https://doi.org/10.1016/j.omtm.2024.101230.

12. Penaud-Budloo, M., François, A., Clément, N., and Ayuso, E. (2018). Pharmacology of Recombinant Adeno-associated Virus Production. Mol. Ther. Methods Clin. Dev. *8*, 166–180. https://doi.org/10.1016/j.omtm.2018.01.002.

13. Colella, P., Ronzitti, G., and Mingozzi, F. (2018). Emerging Issues in AAV-Mediated In Vivo Gene Therapy. Mol. Ther. Methods Clin. Dev. *8*, 87–104. https://doi.org/10.1016/j.omtm.2017.11.007.

14. Philpott, N.J., Giraud-Wali, C., Dupuis, C., Gomos, J., Hamilton, H., Berns, K.I., and Falck-Pedersen, E. (2002). Efficient integration of recombinant adeno-associated virus DNA vectors requires a p5-rep sequence in cis. J. Virol. *76*, 5411–5421. https://doi.org/10.1128/jvi.76.11.5411-5421.2002.

15. Smith, R.H., Levy, J.R., and Kotin, R.M. (2009). A simplified baculovirus-AAV expression vector system coupled with one-step affinity purification yields high-titer rAAV stocks from insect cells. Mol. Ther. *17*, 1888–1896. https://doi.org/10.1038/mt.2009.128.

16. FDA. Chemistry. Manufacturing, and Control (CMC) Information for Human Gene Therapy Investigational New Drug Applications (INDs). https://www.fda.gov/regulatory-information/search-fda-guidance-documents/chemistry-manufacturing-and-control-cmc-information-human-gene-therapy-investigational-new-drug.

17. EMA. Quality, preclinical and clinical aspects of gene therapy medicinal products - Scientific guideline. https://www.ema.europa.eu/en/quality-preclinical-clinical-aspects-gene-therapy-medicinal-products-scientific-guideline.

18. EMA. Quality, non-clinical and clinical issues relating specifically to recombinant adeno-associated viral vectors - Scientific guideline. https://www.ema.europa.eu/en/quality-non-clinical-clinical-issues-relating-specifically-recombinant-adeno-associated-viral-vectors-scientific-guideline.

19. NMPA. Chinese Pharmacopoeia-General Principles for Human Gene Therapy Products. https://ydz.chp.org.cn/#/item?bookId=3&entryId=5354.

20. NMPA. Technical Guidelines for the Evaluation of Recombinant Adeno-associated Viral Vector-based In Vivo Gene Therapy Products in Clinical Trials. https://www.cde.org.cn/main/news/viewInfoCommon/635323ee319dacab26eb783b843b8bd3.

21. Wright, J.F., and Zelenaia, O. (2011). Vector characterization methods for quality control testing of recombinant adeno-associated viruses. Methods Mol. Biol. *737*, 247–278. https://doi.org/10.1007/978-1-61779-095-9_11.

22. Robert, M.A., Chahal, P.S., Audy, A., Kamen, A., Gilbert, R., and Gaillet, B. (2017). Manufacturing of recombinant adeno-associated viruses using mammalian expression platforms. Biotechnol. J. *12*, 1600193. https://doi.org/10.1002/biot.201600193.

23. Yip, M., Chen, J., Zhi, Y., Tran, N.T., Namkung, S., Pastor, E., Gao, G., and Tai, P.W.L. (2023). Querying Recombination Junctions of Replication-Competent Adeno-Associated Viruses in Gene Therapy Vector Preparations with Single Molecule, Real-Time Sequencing. Viruses *15*, 1228. https://doi.org/10.3390/v15061228.

24. Brinkman, E.K., Chen, T., Amendola, M., and van Steensel, B. (2014). Easy quantitative assessment of genome editing by sequence trace decomposition. Nucleic Acids Res. *42*, e168. https://doi.org/10.1093/nar/gku936.

25. Ellis, B.L., Hirsch, M.L., Barker, J.C., Connelly, J.P., Steininger, R.J., 3rd, and Porteus, M.H. (2013). A survey of ex vivo/in vitro transduction efficiency of mammalian primary cells and cell lines with Nine natural adeno-associated virus (AAV1-9) and one engineered adeno-associated virus serotype. Virol. J. *10*, 74. https://doi.org/10.1186/1743-422x-10-74.

26. Meier, A.F., Fraefel, C., and Seyffert, M. (2020). The Interplay between Adeno-Associated Virus and its Helper Viruses. Viruses *12*, 662. https://doi.org/10.3390/v12060662.

27. Hamilton, B.A., Li, X., Pezzulo, A.A., Abou Alaiwa, M.H., and Zabner, J. (2019). Polarized AAVR expression determines infectivity by AAV gene therapy vectors. Gene Ther. *26*, 240–249. https://doi.org/10.1038/s41434-019-0078-3.

28. Song, L.K., Ma, K.L., Yuan, Y.H., Mu, Z., Song, X.Y., Niu, F., Han, N., and Chen, N. H. (2015). Targeted Overexpression of α-Synuclein by rAAV2/1 Vectors Induces Progressive Nigrostriatal Degeneration and Increases Vulnerability to MPTP in Mouse. PLoS One *10*, e0131281. https://doi.org/10.1371/journal.pone.0131281.

29. Sørensen, A.T., Kanter-Schlifke, I., Lin, E.J.D., During, M.J., and Kokaia, M. (2008). Activity-dependent volume transmission by transgene NPY attenuates glutamate release and LTP in the subiculum. Mol. Cell. Neurosci. *39*, 229–237. https://doi.org/10.1016/j.mcn.2008.06.014.

30. Meng, J.S., He, Y., Yang, H.B., Zhou, L.P., Wang, S.Y., Feng, X.L., Yahya Al-Shargi, O., Yu, X.M., Zhu, L.Q., and Ling, C.Q. (2024). Melittin analog p5RHH enhances recombinant adeno-associated virus transduction efficiency. J. Integr. Med. *22*, 72–82. https://doi.org/10.1016/j.joim.2024.01.001.

31. Zhu, X., Yang, K., Xie, J., Feng, X., Wu, T., Hu, M., Wang, H., Yu, C., Yu, X., Hemmatzadeh, F., et al. (2025). An SDS-NaOH-based method to isolate genome of recombinant adeno-associated virus vectors for physical titer measurement. PLoS One *20*, e0315921. https://doi.org/10.1371/journal.pone.0315921.

32. Luo, J., Deng, Z.L., Luo, X., Tang, N., Song, W.X., Chen, J., Sharff, K.A., Luu, H.H., Haydon, R.C., Kinzler, K.W., et al. (2007). A protocol for rapid generation of recombinant adenoviruses using the AdEasy system. Nat. Protoc. *2*, 1236–1247. https://doi.org/10.1038/nprot.2007.135.

33. Stemmer, M., Thumberger, T., Del Sol Keyer, M., Wittbrodt, J., and Mateo, J.L. (2015). CCTop: An Intuitive, Flexible and Reliable CRISPR/Cas9 Target Prediction Tool. PLoS One *10*, e0124633. https://doi.org/10.1371/journal.pone.0124633.

34. Kafri, T., Blömer, U., Peterson, D.A., Gage, F.H., and Verma, I.M. (1997). Sustained expression of genes delivered directly into liver and muscle by lentiviral vectors. Nat. Genet. *17*, 314–317. https://doi.org/10.1038/ng1197-314.